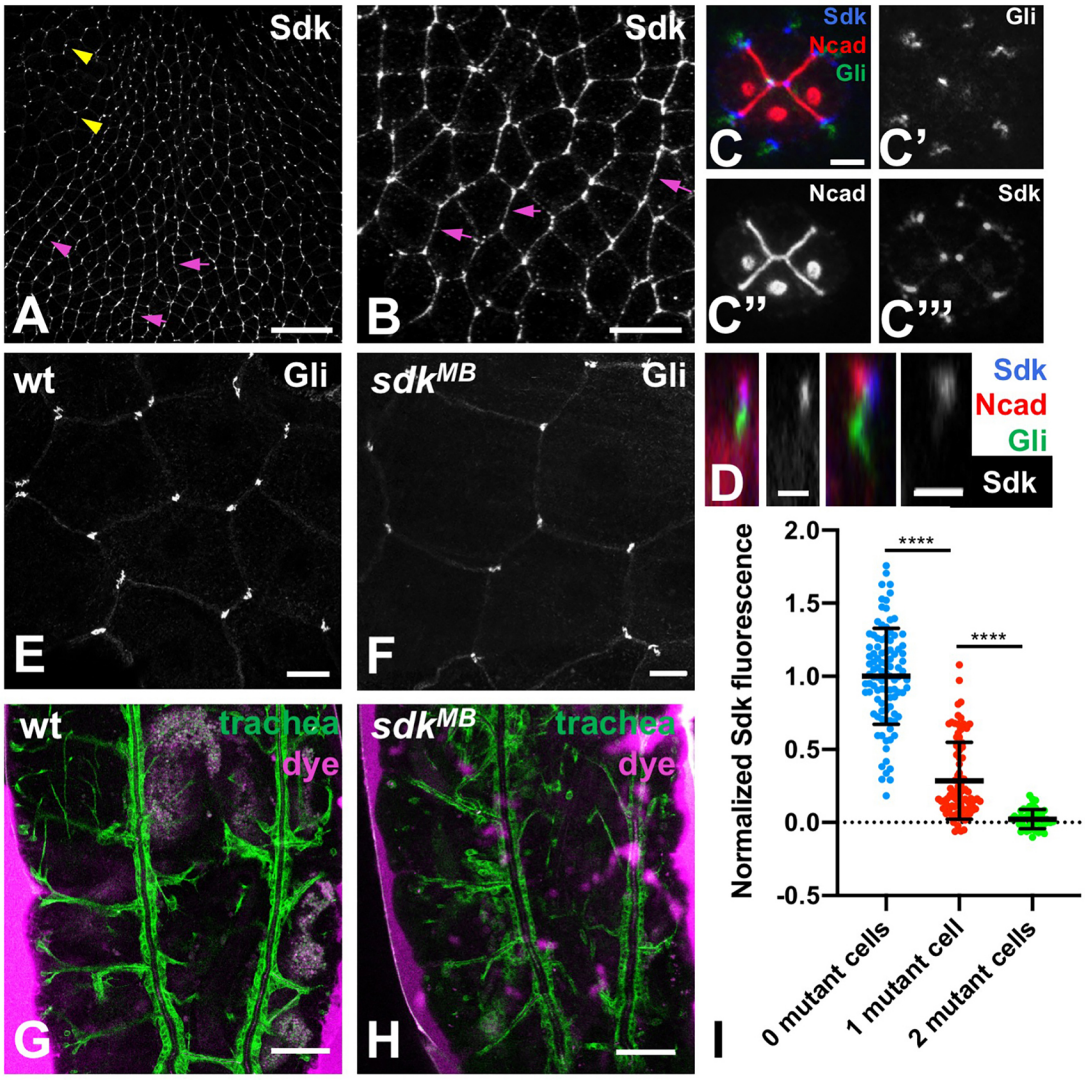

Letizia et al. Figure S1

Figure S1, related to Figure 1: *sdk* does not affect tricellular septate junctions. (A, B) Sdk staining in a stage 7 embryo. Sdk is strongly enriched at vertices in the dorsal epidermis (yellow arrows), but shows planar polarized accumulation at bicellular anterior-posterior cell contacts (purple arrows). (B) is an enlargement of the ventral region. n=10. (C, D) wild type 42 h pupal retina stained for Gli (green, C'), Ncad (red, C'') and Sdk (blue, C''', white in D). (C) shows a single ommatdium and (D) two xz projections. n=18. Sdk is at the same apical-basal level as Ncad and either overlapping or adjacent to it. (E, F) show the epidermis of wild type (E) and $sdk^{MB05054}$ (F) third instar larvae, stained for Gli. n=6 (wt) or 2 (*sdk*). Gli is correctly localized to tricellular junctions in *sdk* mutants. (G, H) show stage 17 *btl-GAL4, UAS-Src-GFP* (G) and $sdk^{MB05054}$; *btl-GAL4, UAS-Src-GFP* (H) embryos after dye injection. n=5 of each genotype. Tracheal cells can be directly visualized by the presence of GFP. Dye (magenta) is present in the body cavity, but does not enter the tracheal lumen. (I) Quantification of Sdk fluorescence intensity at tAJs with 0, 1 or 2 $sdk^{\Delta 15}$ mutant cells in clones in 42 h pupal retina. n=98 tAJs (0 mutant cells), 86 tAJs (1 mutant cell) or 49 tAJs (2 mutant cells), from 4 retinas. Bars show mean ± SD. ****, $p<0.0001$, unpaired t-test with Welch's correction. Scale bars, 25 μm (A), 10 μm (B, E, F, G, H), or 2 μm (C, D).

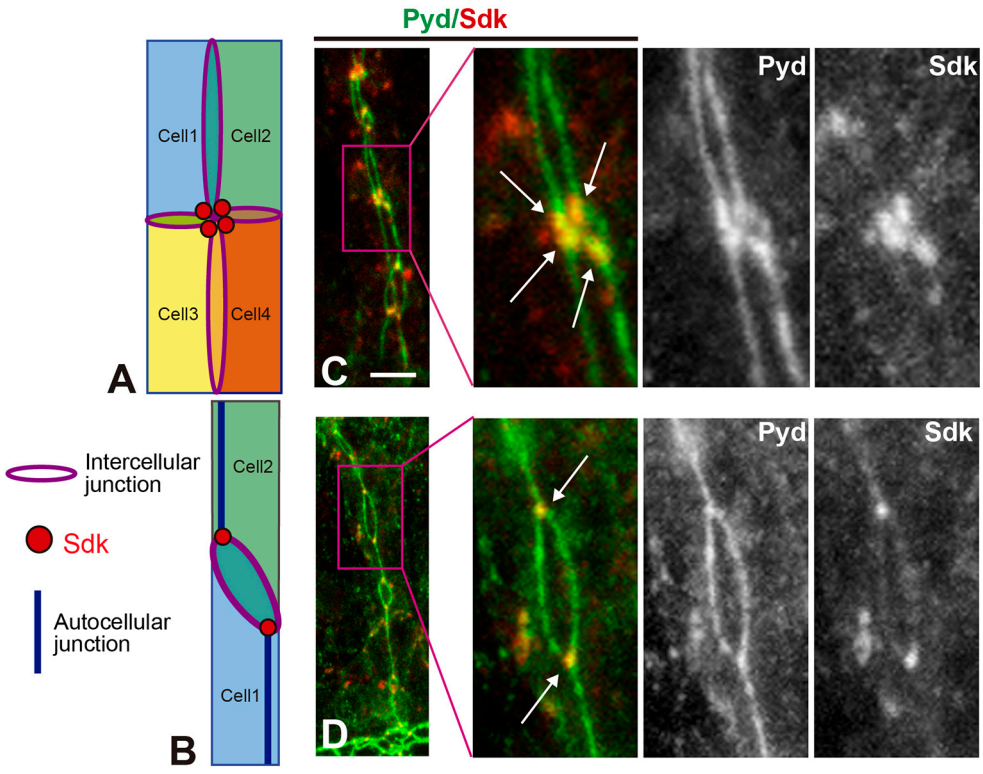

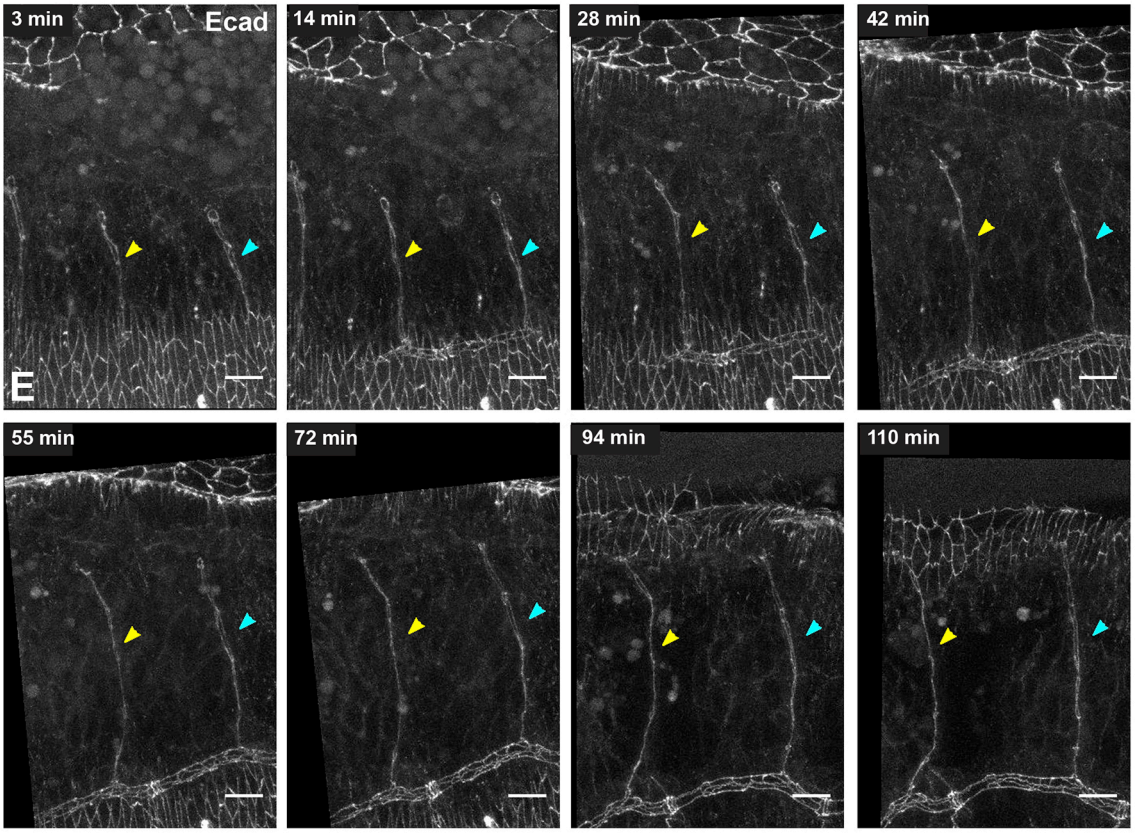

Letizia et al. Figure S2

Figure S2, related to Figure 3: Sdk is localized to autocellular-intercellular vertices during tracheal cell intercalation and is required for proper intercalation. (A, B) diagrams of tracheal cells during the intercalation process. (A) shows an early stage in which cells are positioned in pairs and connected by intercellular junctions. (B) shows two intercalating cells in the process of exchanging intercellular junctions (purple rings) with autocellular junctions (dark blue lines), which corresponds to the zipping up process. Sdk, in red, localizes to cell-cell contacts in (A) and to the boundaries between each zipping autocellular junction and the intercellular junction shared with the next cell in (B). Intercalation can be visualized by staining with junctional markers. (C, D) show projections of confocal sections of embryos at early stage 14 (C, at the beginning of the intercalation process) and late stage 14 (D, during the zipping up process) stained for Pyd (green) and Sdk (red). Boxed regions are enlarged to the right to show details of the intercalation process. Sdk localizes to cell-cell contacts and in intercalating branches it localizes to the vertices between autocellular and intercellular junctions (white arrows). n=20. (E) Still images from a *sdk*^{MB05054}; *Ecad-GFP* embryo imaged during the process of cell intercalation (from early stage 14 to stage 15), focused on two dorsal branches (shown in Movie S1). Yellow arrowheads point to a normal intercalation event in a dorsal branch. Blue arrowheads point to a defective intercalation event where two cells in the dorsal branch maintain an intercellular junction at the end of branch extension. Scale bars, 5 μm (C), 10 μm (E).

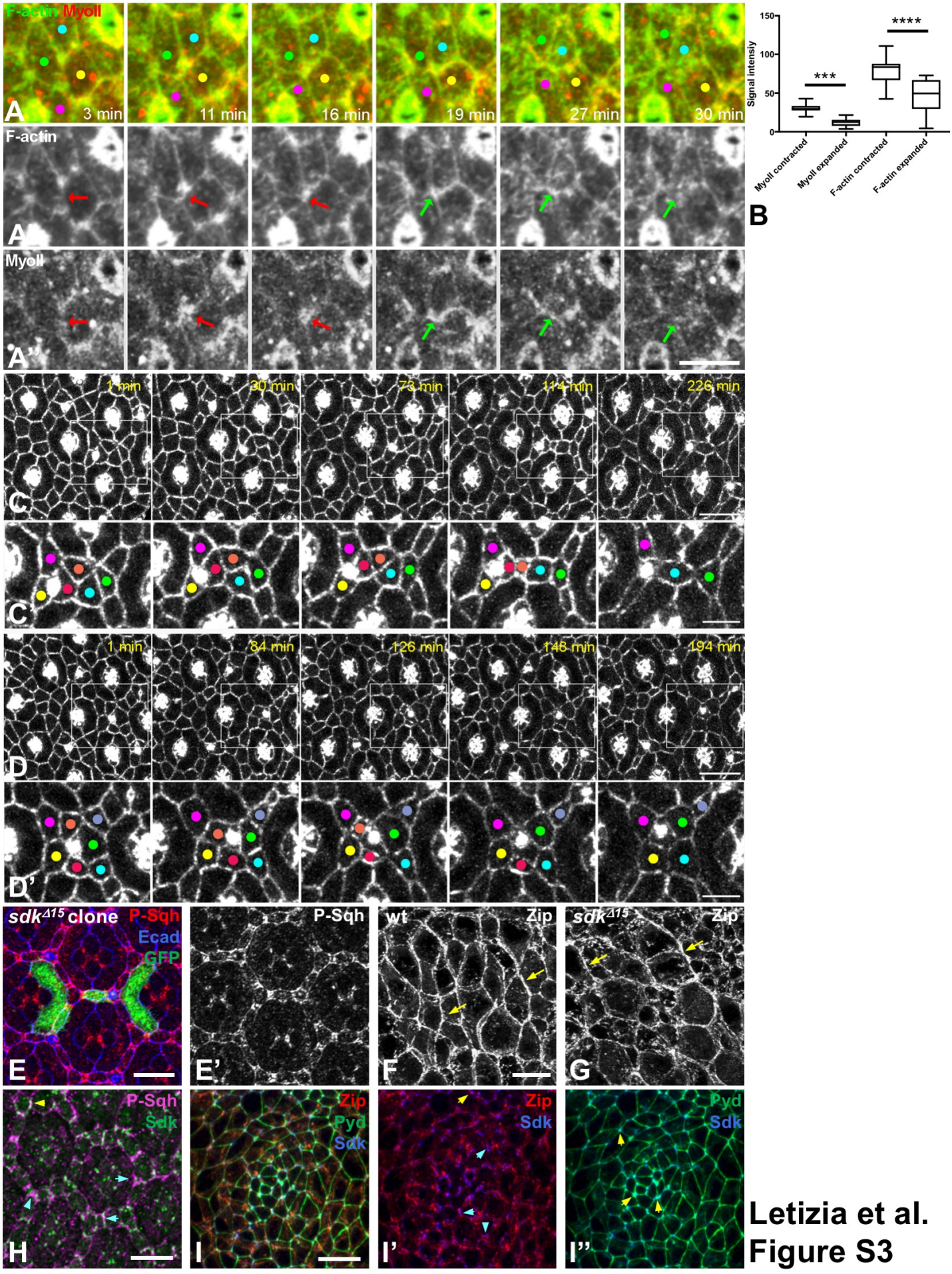

Letizia et al.
Figure S3

Figure S3, related to Figure 3: Sdk affects cell intercalation in the retina. (A) Still images from a LifeAct-GFP (green, A'); Sqh-mCherry (red, A'') pupal retina imaged at 26-27 h APF (shown in Movie S2) focusing on an intercalation event between the four cells indicated by colored dots. Red arrows indicate the shrinking and green arrows the expanding bicellular junction. Shrinkage correlates with recruitment of both actin and myosin, while expansion correlates with loss of these proteins. The initial expansion occurs before actin and myosin are completely lost, suggesting that it may be non-autonomously driven by contraction of neighboring contacts. n=4. (B) Quantification from these movies of the levels of Myosin II and F-actin at contacts during peak contraction that disassembles the contact and during peak expansion that assembles a new contact. Box and whiskers plot shows median, upper and lower quartiles, and upper and lower extremes. n=15 T1 transitions. ***, $p<0.001$; ****, $p<0.0001$ by repeated measures ANOVA followed by post-hoc parametric two-tailed unpaired t-test. (C, D) Still images from a $sdk^{\Delta 15}$ α-catenin-GFP pupal retina imaged at 26-30h APF (shown in Movie S3) to highlight the remodeling of cell-cell contacts in ommatidia with (C) normal (at 1,30,73,114,226 minutes) and (D) abnormal (1,84,126,148,194 minutes) cell intercalation. (C', D') show enlargements of ommatidial edges that are demarcated in boxes in upper panels. Individual cells are marked with colored dots; note that excess cells are lost by apoptosis during this remodeling process. n=4. (E) $sdk^{\Delta 15}$ clone in a 42h APF retina labeled with GFP and stained for phosphorylated Sqh (P-Sqh) (E', red) and Ecad (blue). P-Sqh is not visibly affected in *sdk* mutant cells. n=14. (F, G) wild type (F) and $sdk^{\Delta 15}$ (G) stage 7 embryos stained for Zipper (Zip) myosin heavy chain. Myosin cables along the AP bonds (arrows) are still present in *sdk* mutants. n=9 (wt), n=6 (*sdk*). (H) 42 h APF retina stained for P-Sqh (magenta) and Sdk (green). n=12. (I) Stage 10 embryo stained for Sdk (blue), Zip (red) and Pyd (green). n=6. Note the colocalisation of Sdk and Pyd at vertices (yellow arrows). While Sdk can partially or fully colocalize with P-Sqh and Zip (yellow arrows), they more often display a complementary pattern (blue arrows). In the retina, 12% of junctions show full colocalization of Sdk and P-Sqh, 32% show partial colocalization and 56% show a complementary pattern (n=407 tAJs from 8 retinas). In the embryo, 24% of junctions show full colocalization of Sdk and Zip, 22% show partial colocalization and 52% show a complementary pattern (n=329 tAJs from 6 embryos). Scale bars, 10 μm (A, C, D, E, F, G, H), 7.5 μm (I).

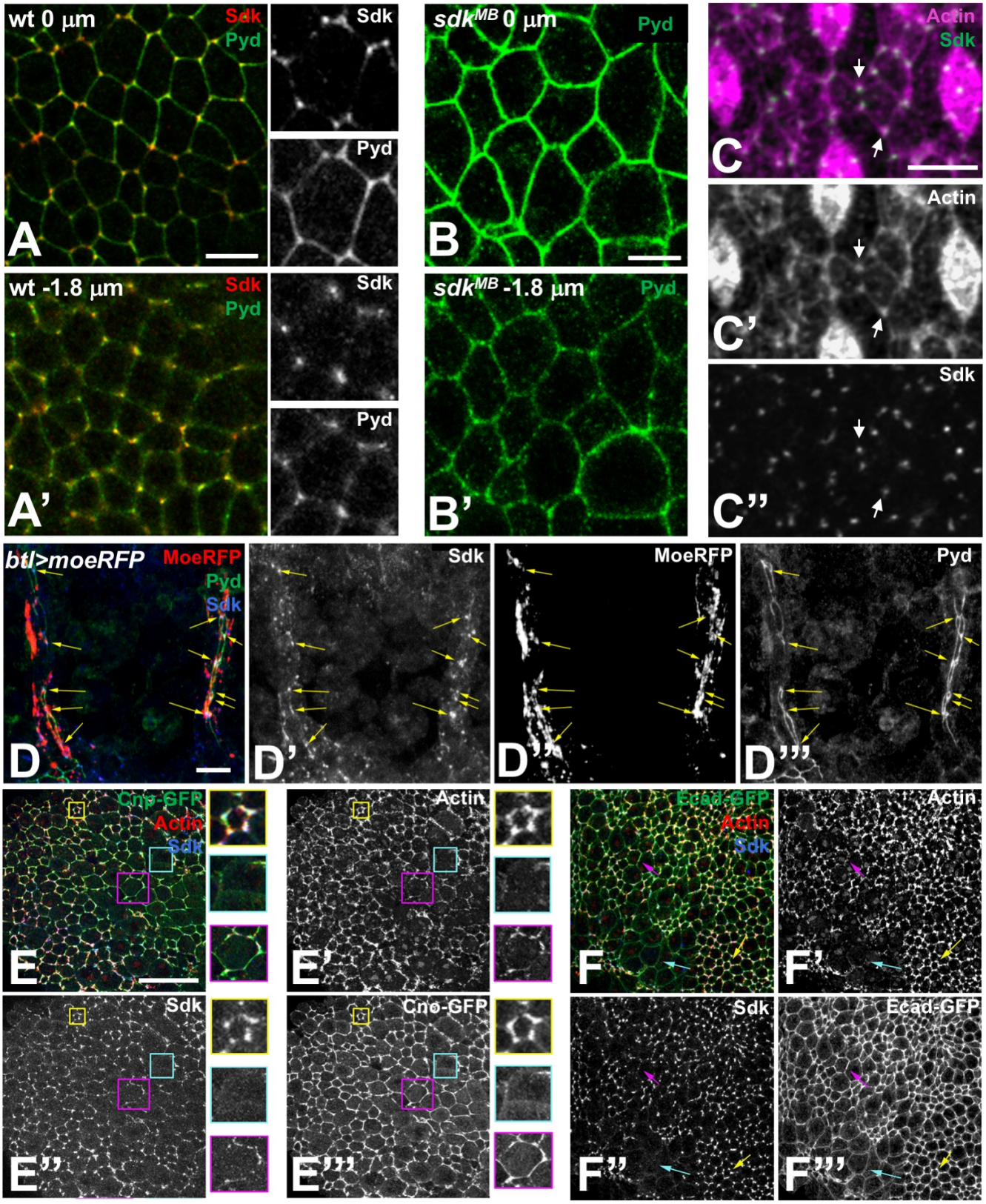

Letizia et al. Figure S4

Figure S4, related to Figure 5: Sdk colocalizes with Pyd and actin and is affected by actin depolymerization. (A) lateral view of a wild type stage 9 embryo, stained for Pyd (green) and Sdk (red). An enlargement is shown to the right. (A) shows the apical surface and (A') is 1.8 μm below the apical surface. Pyd is enriched at tAJs subapically, where it colocalizes with Sdk. (B) *sdk*^{MB05054} stage 9 embryo showing Pyd staining apically (B) and 1.8 μm subapically (B'). Pyd is not enriched at tAJs in *sdk* mutants. Quantifications are shown in Fig. 5F. (C) still image from a movie of retinal intercalation showing Sdk-GFP (C'', green) and Utrophin-mCherry driven by the *sqh* promoter, which labels actin (C', magenta). Actin is enriched in a spot at tricellular vertices, where it colocalizes with Sdk (arrows). At this stage, Sdk enrichment at tAJs is 15.0 ± 4.5, and actin enrichment at tAJs is 6.2 ± 1.6 (mean ± S.E.M., n=30 tAJs from 4 movies). (D) shows tracheal branches in a late stage 14 embryo expressing *UAS-moesinRFP* with *btl-GAL4* to mark actin filaments (D'', red), stained for Sdk (D', blue) and Pyd (D''', green). Sdk and Pyd colocalize with actin (arrows). n=10. (E, F) Cno-GFP (E) and Ecad-GFP (F) stage 9/10 embryos treated with 5 μM Latrunculin A for 40 min and stained for Actin (E', F', red), Sdk (E'', F'', blue) and GFP (E''', F''', green). Enlargements of the boxed regions in (E) are shown to the right. The Latrunculin A treatment had a non-uniform effect, producing regions in the epithelium with almost normal actin (yellow boxes and arrows), regions with reduced and/or fragmented actin (pink boxes and arrows) and regions with no detectable actin (blue boxes and arrows). Sdk and Cno are not affected in regions with normal actin and the three proteins are enriched in the vertices (yellow). In contrast, Sdk is decreased and diffuses along the bAJs (pink) when actin is disorganized. When actin is absent, Sdk and Cno are completely lost from junctions, although Ecad is still present (blue). n=8 (E) or 7 (F). Scale bars, 5 μm (A-D), 25 μm (E, F).

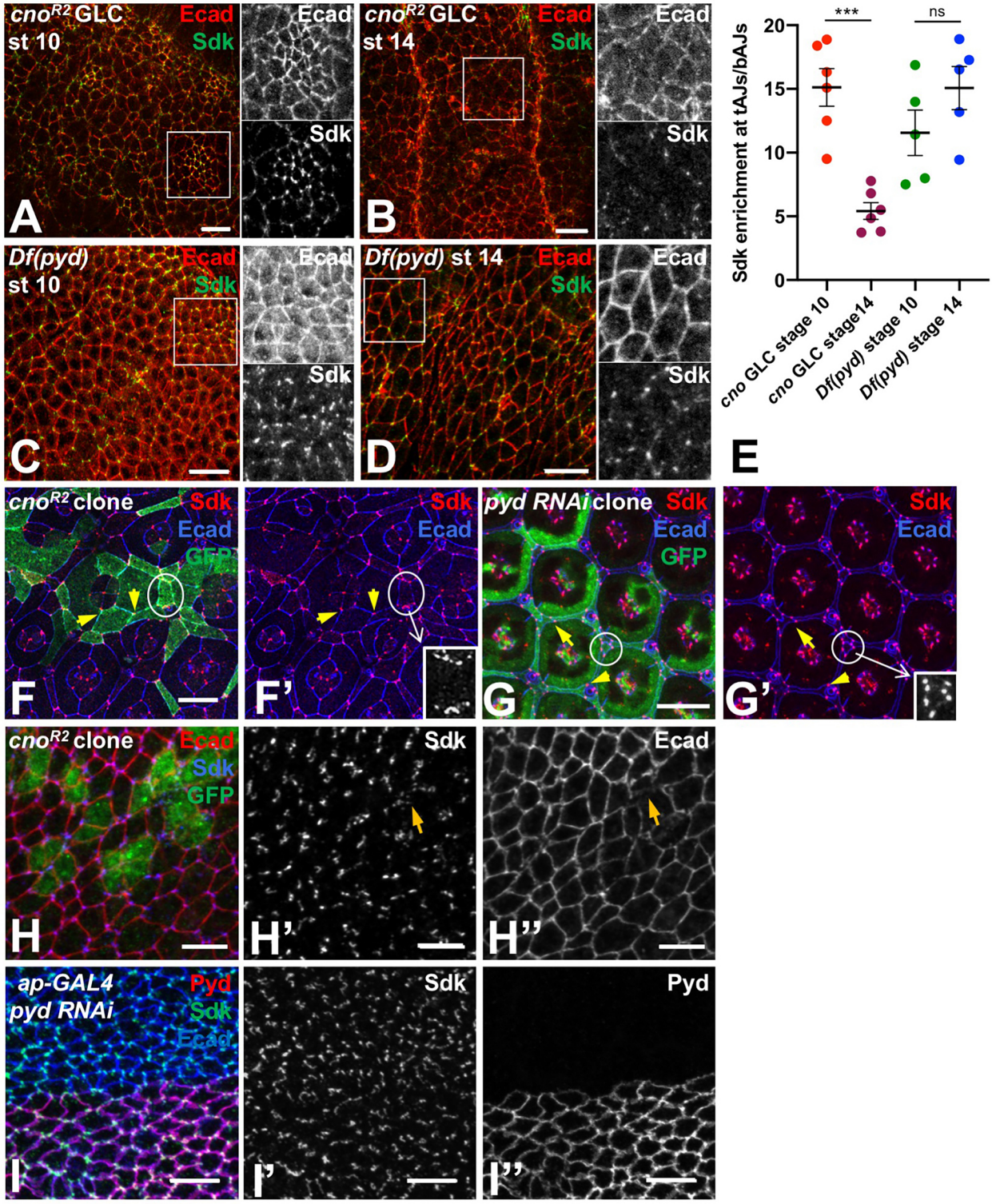

Letizia et al. Figure S5

Figure S5, related to Figure 5: Cno and Pyd are not essential for Sdk localization to tAJs. (A-D) *cno*^{R2} maternal-zygotic mutant (A, B) or *Df(pyd)* (C, D) stage 10 (A, C) or 14 (B, D) embryos, stained for Sdk (green) and Ecad (red). Single-channel enlargements of the boxed regions are shown to the right. Sdk is localized correctly to most tAJs in *cno* mutants at stage 10 and in *pyd* mutants at both stages, but is reduced at tAJs concomitantly with Ecad in stage 14 *cno* mutants. (E) is a quantification of Sdk enrichment at tAJs relative to bAJs in these genotypes and stages. n=6 (*cno* stage 10 and 14) or 5 (*pyd* stage 10 and 14), with each point being the mean of 10-15 cells from one embryo. Bars show mean ± SEM. ***, p=0.0001, ns, not significant by unpaired t-test. (F, G) show 42 h APF pupal retinas with *cno*^{R2} clones (F) or *pyd RNAi* clones (G) marked with GFP (green), stained for Sdk (red) and Ecad (blue). n=14 (*cno*), n=8 (*pyd*). Sdk still localizes to many tAJs within the clones (arrows show examples). Sdk staining in the circled cells is enlarged in the insets. (H, I) show wing imaginal discs with *cno*^{R2} clones marked with GFP (green, H) or expressing *pyd RNAi* with *ap-GAL4* (I) stained for Sdk (H', I', blue in H, green in I), Ecad (H'', red in H, blue in I) and Pyd (F'', red in I). n=17 (*cno*), n=8 (*pyd*). Sdk is more diffusely localized along bAJs on which Ecad is reduced within the *cno* clone (arrow), but is correctly localized in cells expressing *pyd RNAi*. Scale bars, 10 μm.

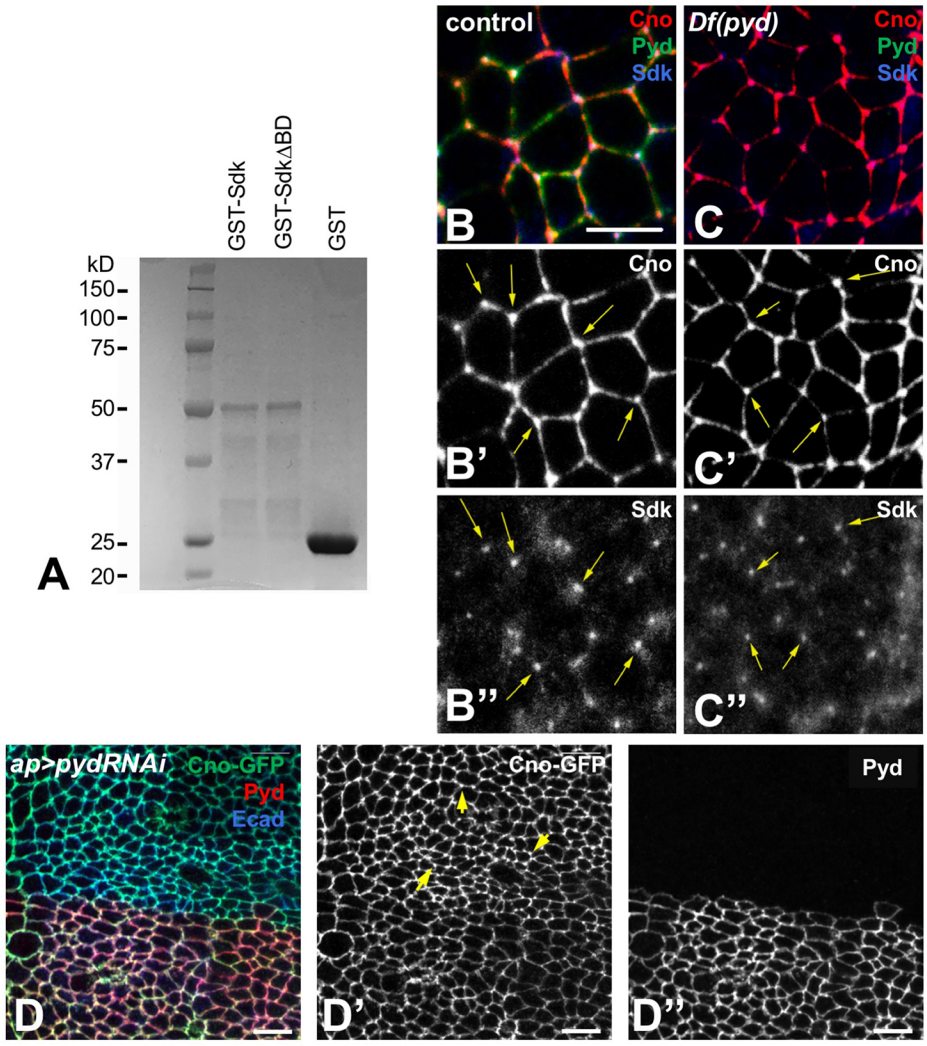

Letizia et al. Figure S6

Figure S6, related to Figure 6: Pyd does not localize Cno to tAJs. (A) Coomassie-stained gel of GST proteins, showing equal expression of GST-Sdk and GST-SdkΔBD. n=3. (B, C) stage 11 wild type (B) or *Df(pyd)* (C) embryos stained for Cno (B', C', red), Sdk (B'', C'', blue) and Pyd (green). n=3 (wt), n=5 (*pyd*). Sdk is present and Cno is enriched at tAJs in both control and *pyd* mutant embryos (arrows). (D) shows a wing disc expressing *pyd* RNAi in the dorsal domain with *apterous-GAL4*, stained for Cno-GFP (D', green), Pyd (D'', red) and Ecad (blue). n=17. Cno-GFP still localizes to tAJs in regions with no detectable Pyd (arrows).